nature genetics

NMNAT1 mutations cause Leber congenital amaurosis

Marni J Falk[1,2,22], Qi Zhang[3,4,22], Eiko Nakamaru-Ogiso[5], Chitra Kannabiran[6], Zoe Fonseca-Kelly[3,4], Christina Chakarova[7], Isabelle Audo[8–11], Donna S Mackay[7], Christina Zeitz[8–10], Arundhati Dev Borman[7,12], Magdalena Staniszewska[3,4], Rachna Shukla[6], Lakshmi Palavalli[6], Saddek Mohand-Said[8–11], Naushin H Waseem[7], Subhadra Jalali[6,13], Juan C Perin[14], Emily Place[1,3,4], Julian Ostrovsky[1], Rui Xiao[15], Shomi S Bhattacharya[7,16], Mark Consugar[3,4], Andrew R Webster[7,12], José-Alain Sahel[8–11,17,18], Anthony T Moore[7,12,19], Eliot L Berson[4], Qin Liu[3,4], Xiaowu Gai[20,21,23] & Eric A Pierce[3,4,23]

Leber congenital amaurosis (LCA) is an infantile-onset form of inherited retinal degeneration characterized by severe vision loss[1,2]. Two-thirds of LCA cases are caused by mutations in 17 known disease-associated genes[3] (Retinal Information Network (RetNet)). Using exome sequencing we identified a homozygous missense mutation (c.25G>A, p.Val9Met) in *NMNAT1* that is likely to be disease causing in two siblings of a consanguineous Pakistani kindred affected by LCA. This mutation segregated with disease in the kindred, including in three other children with LCA. *NMNAT1* resides in the previously identified LCA9 locus and encodes the nuclear isoform of nicotinamide mononucleotide adenylyltransferase, a rate-limiting enzyme in nicotinamide adenine dinucleotide (NAD^+) biosynthesis[4,5]. Functional studies showed that the p.Val9Met alteration decreased NMNAT1 enzyme activity. Sequencing *NMNAT1* in 284 unrelated families with LCA identified 14 rare mutations in 13 additional affected individuals. These results are the first to link an NMNAT isoform to disease in humans and indicate that *NMNAT1* mutations cause LCA.

Inherited retinal diseases, such as LCA, represent a heterogeneous group of early-onset blindness disorders that are characterized by progressive dysfunction and death of the rod and cone retinal photoreceptor cells[6]. Despite the identification so far of more than 180 different inherited retinal disease–associated genes, the genetic etiology remains uncertain in 40–50% of individuals with inherited retinal disease[7] (RetNet). Additional loci have been identified at which disease-associated genes have not yet been identified, such as the LCA9 locus mapped to chromosome 1p36 (ref. 4). Identifying the genetic basis of inherited retinal diseases is essential to guide the development of potential therapies, as highlighted by the recent success of clinical gene therapy trials for *RPE65*-related LCA[8–12]. Here, we used whole-exome sequencing in a large consanguineous Pakistani family, including five children affected with LCA who did not have mutations in known LCA-causing genes.

Two Pakistani siblings, an 11-year-old girl and her 3-year-old brother (**Fig. 1a**, family 047, subjects IV-1 and IV-3, respectively), initially came to the Ophthalmology-Genetics Clinic at the Children's Hospital of Philadelphia for evaluation of LCA because of severe vision impairment, congenital nystagmus and no detectable (<10 μV) retinal function by full-field electroretinography (ERG) testing in early infancy (see **Supplementary Note** for additional clinical details). Both children also had global developmental delay, nonverbal autism with stereotypies, hypotonia with joint hypermobility and dysmorphic facies. Severe-to-profound bilateral sensorineural hearing loss was present in the 11-year-old proband (IV-1) and in her 8-year-old brother (IV-2), who had a normal eye exam and normal development but exhibited clinical features consistent with mucolipidosis (**Supplementary Note**).

[1]Department of Pediatrics, Division of Human Genetics, The Children's Hospital of Philadelphia and University of Pennsylvania Perelman School of Medicine, Philadelphia, Pennsylvania, USA. [2]Department of Pediatrics, Division of Child Development and Metabolic Disease, The Children's Hospital of Philadelphia and University of Pennsylvania Perelman School of Medicine, Philadelphia, Pennsylvania, USA. [3]Department of Ophthalmology, Ocular Genomics Institute, Massachusetts Eye and Ear Infirmary, Harvard Medical School, Boston, Massachusetts, USA. [4]Berman-Gund Laboratory for the Study of Retinal Degenerations, Department of Ophthalmology, Massachusetts Eye and Ear Infirmary, Harvard Medical School, Boston, Massachusetts, USA. [5]Department of Biochemistry and Biophysics, University of Pennsylvania Perelman School of Medicine, Philadelphia, Pennsylvania, USA. [6]Kallam Anji Reddy Molecular Genetics Laboratory, LV Prasad Eye Institute (LVPEI), Kallam Anji Reddy Campus, LV Prasad Marg, Hyderabad, India. [7]Institute of Ophthalmology, University College of London, London, UK. [8]Institut National de la Santé et de la Recherche Médicale (INSERM) U968, Paris, France. [9]Université Pierre et Marie Curie (UPMC Paris 06), Unité Mixte de Recherche (UMR)_S 968, Institut de la Vision, Paris, France. [10]Centre National de la Recherche Scientifique, UMR 7210, Paris, France. [11]Centre Hospitalier National d'Ophtalmologie des Quinze-Vingts, INSERM–Direction de l'Hospitalisation et de l'Organisation des Soins (DHOS) Centre d'Investigation Clinique 503, Paris, France. [12]Moorfields Eye Hospital, London, UK. [13]Srimati Kanuri Santhamma Centre for Vitreoretinal Diseases, LVPEI, Kallam Anji Reddy Campus, LV Prasad Marg, Hyderabad, India. [14]Center for Biomedical Informatics, Children's Hospital of Philadelphia, Philadelphia, Pennsylvania, USA. [15]Department of Biostatistics and Epidemiology, University of Pennsylvania Perelman School of Medicine, Philadelphia, Pennsylvania, USA. [16]Centro Andaluz de Biología Molecular y Medicina Regenerativa (CABIMER), Isla de Cartuja, Seville, Spain. [17]Fondation Ophtalmologique Adolphe de Rothschild, Paris, France. [18]Académie des Sciences–Institut de France, Paris, France. [19]Great Ormond Street Hospital for Children, London, UK. [20]Department of Molecular Pharmacology and Therapeutics, Loyola University Chicago Health Sciences Division, Maywood, Illinois, USA. [21]Center for Biomedical Informatics, Loyola University Chicago Health Sciences Division, Maywood, Illinois, USA. [22]These authors contributed equally to this work. [23]These authors jointly directed this work. Correspondence should be addressed to E.A.P. (eric_pierce@meei.harvard.edu).

Received 12 February; accepted 29 June; published online 29 July 2012; doi:10.1038/ng.2361

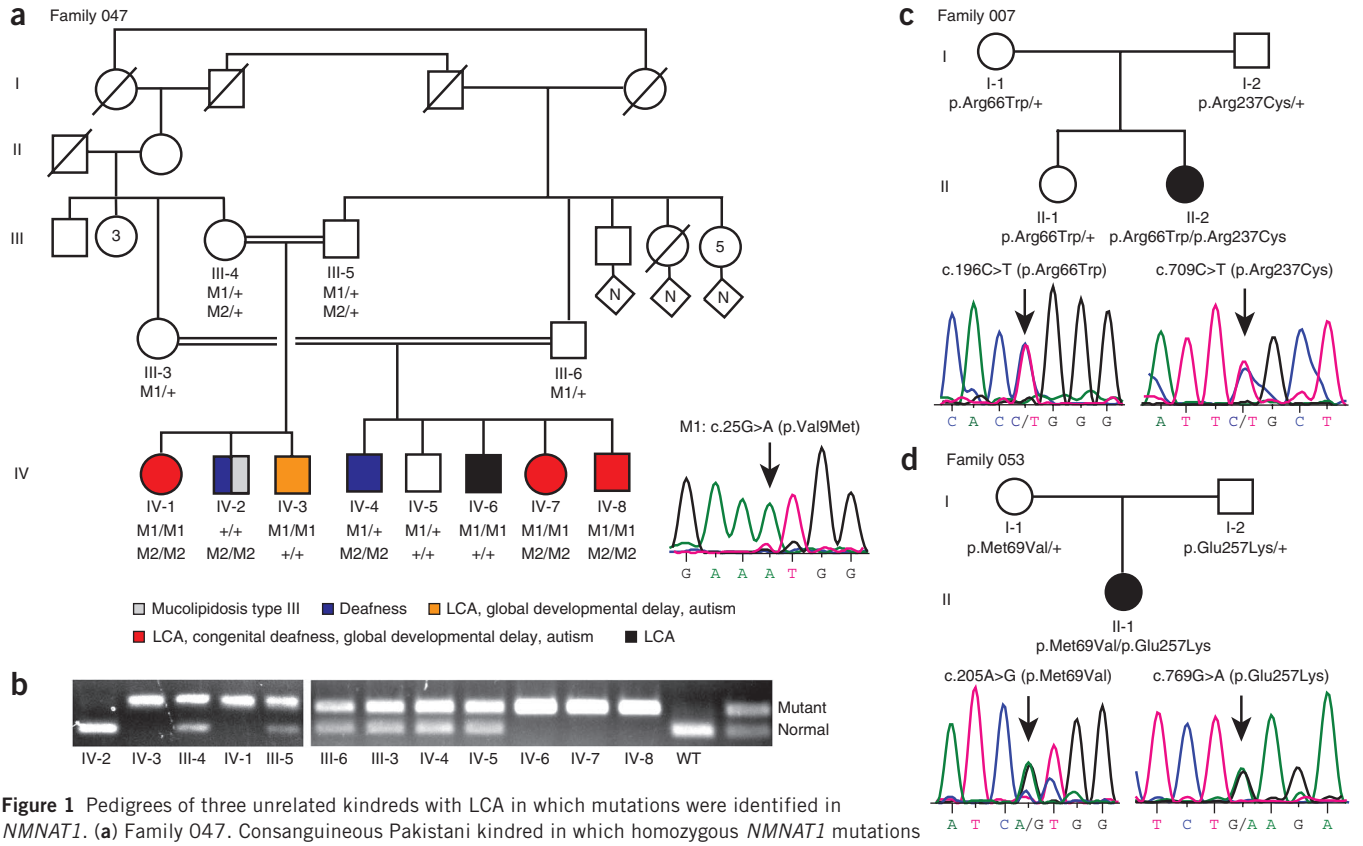

Figure 1 Pedigrees of three unrelated kindreds with LCA in which mutations were identified in *NMNAT1*. (**a**) Family 047. Consanguineous Pakistani kindred in which homozygous *NMNAT1* mutations were identified in five children with LCA by whole-exome sequencing with validation by Sanger sequencing. M1, *NMNAT1* mutation (c.25G>A, p.Val9Met); M2, *GJB2* mutation (c.71G>A, p.Trp24*). A representative sequence trace for M1 is shown. Colored symbols indicate affected individuals. Numbers within symbols indicate multiple offspring of a given gender. Diamonds represent individuals of unknown gender, and N indicates multiple individuals of unknown number. Slashes indicate deceased individuals. (**b**) Genotyping of family 047. Members were genotyped by PCR amplification of exon 2 of *NMNAT1*, and PCR products were digested with AcuI to distinguish wild-type and mutant sequences (sizes of digested wild-type and mutant products shown in the last lane). (**c**) Family 007. A single proband with LCA was shown by Sanger sequencing of *NMNAT1* to harbor compound heterozygous mutations c.196C>T (p.Arg66Trp) and c.709C>T (p.Arg237Cys). (**d**) Family 053. A single proband with LCA was shown by Sanger sequencing of *NMNAT1* to harbor compound heterozygous mutations c.205A>G (p.Met69Val) and c.769G>A (p.Glu257Lys). +, wild type. Sample sequence traces are shown in **c** and **d**.

Their parents were first cousins who were visually and developmentally normal (**Fig. 1a**, subjects III-4 and III-5). Notably, the parents' siblings had married one another (**Fig. 1a**, subjects III-3 and III-6) and together had two children with similar vision and nonverbal autism phenotypes as the proband (subjects IV-7 and IV-8) and one child with isolated LCA (IV-6). Clinical genetic diagnostic testing identified a homozygous mutation in *GJB2* (c.71G>A, p.Trp24*) as the cause of sensorineural hearing loss in subject IV-1, but no mutation was identified in any of the known LCA-causing genes (**Supplementary Note**). Additional sequencing analyses verified that the homozygous mutation encoding p.Trp24* in GJB2 segregated with the hearing loss phenotype in the larger kindred (**Fig. 1a**).

To search for the genetic cause of LCA in this family, we performed whole-exome sequencing of the nuclear family of the 11-year-old proband (**Fig. 1a**, subjects IV-1, IV-2, IV-3, III-4 and III-5). Given known consanguinity, a homozygous mutation of biparental inheritance that was shared by both affected children but not by their sibling with normal visual acuity was postulated to be the most likely mode of LCA inheritance. We identified a total of 113 nonsynonymous variants in 86 genes that met these criteria (**Supplementary Fig. 1**). Four of these variants were rare or novel according to dbSNP 132, 1000 Genomes Project data and National Heart, Lung, and Blood Institute (NHLBI) Exome Sequencing Project (ESP) data[13,14]. The genes harboring these four variants had known retinal expression, which was determined from mouse retina RNA sequencing (RNA-seq) analyses[15]. Only one of these variants was predicted to damage protein function by SIFT, PolyPhen-2 and other programs: c.25G>A (p.Val9Met) in *NMNAT1* (refs. 16–20) (NM_022787). Sanger sequencing of the c.25G>A variant in *NMNAT1* validated its segregation with the LCA phenotype in the original nuclear kindred and in the proband's similarly affected cousins, including the one with isolated LCA (**Fig. 1a**,**b**). Only the mutant M1 allele encoding p.Val9Met NMNAT1 was detected in the five children with LCA in generation IV, whereas the four unaffected parents of these children in generation III carry both the mutant and wild-type alleles, and their three children with normal vision harbor only the wild-type allele (**Fig. 1b**). The p.Val9Met variant was not present in 501 controls or in any public databases[13,14].

No clearly pathogenic mutations were identified that were likely to be the cause of developmental delay, nonverbal autism, hypotonia and dysmorphic facies in family members IV-1, IV-3, IV-7 and IV-8. These presentations likely have a separate genetic etiology from that of LCA and deafness in this family, as individual IV-6 has LCA alone, individual IV-2 has deafness alone and additional *NMNAT1* mutations were identified in individuals with non-syndromic LCA, as described below.

Table 1 Identified *NMNAT1* mutations

	Ancestry or nationality	Alterations		EVS[a]	PolyPhen-2[b]	SIFT[c]
		DNA	Protein			
CHOP/MEEI						
LCA-047	Pakistani	c.25G>A	p.Val9Met (homo)	Novel	PoD	D
LCA-007	Asian American	c.196C>T	p.Arg66Trp	Novel	PrD	D
		c.709C>T	p.Arg237Cys	1/7,019	PrD	D
LCA-053	African American	c.205A>G	p.Met69Val	Novel	PrD	D
		c.769G>A	p.Glu257Lys[d]	13/10,745	B	T
LVPEI						
LCA-73	Indian	c.25G>A	p.Val9Met (homo)	Novel	PoD	D
LCA-79	Indian	c.98A>G	p.Asp33Gly (homo)	Novel	PrD	D
LCA-100	Indian	c.709C>T	p.Arg237Cys	Novel	PrD	D
		c.565delG	p.Ala189Leufs*25	1/7,019		
LCA-128	Indian	c.215T>A	p.Leu72His (homo)	Novel	PrD	D
UCL						
LCA-1	European descent	c.205A>G	p.Met69Val	Novel	PrD	D
		c.769G>A	p.Glu257Lys	13/10,745	B	T
LCA-2	Caribbean, Sri Lankan	c.161C>T	p.Ala54Val	1/10,757	PrD	D
		c.293T>G	p.Val98Gly	Novel	PrD	T
LCA-3	Caribbean	c.37G>A	p.Ala13Thr	1/10,757	PrD	D
		c.293T>G	p.Val98Gly	11/10,747	PrD	T
LCA-4	Caribbean, Irish	c.723delA	p.Pro241Profs*45	Novel	N/A	N/A
		c.769G>A	p.Glu257Lys	13/10,745	B	T
LCA-5	Polish	c.59T>A	p.Ile20Asn	Novel	PrD	D
		c.769G>A	p.Glu257Lys	13/10,745	B	T
LCA-6	British (European descent)	c.552A>G	p.Ile184Met	Novel	PoD	D
		c.769G>A	p.Glu257Lys	13/10,745	B	T
LCA-7	British (European descent)	c.466G>C	p.Gly156Arg	Novel	PrD	D
		c.769G>A	p.Glu257Lys	13/10,745	B	T

CHOP, Children's Hospital of Philadelphia; LVPEI, LV Prasad Eye Hospital; MEEI, Massachusetts Eye and Ear Infirmary; UCL, University College London.

[a]Data from Exome Variant Server, number of times variant detected/number of exomes analyzed. [b]PolyPhen-2 Hum-Var score: PrD, probably damaging; PoD, possibly damaging; B, benign. [c]SIFT: D, damaging; T, tolerated; N/A, not applicable. [d]The p.Glu257Lys variant in NMNAT1 was detected in a total of six families. Although this variant is sufficiently rare to be associated with LCA (estimated prevalence of 1 in 30,000)[33] according to ESP data (13/10,745 = 0.12%), it is not predicted to damage protein function by PolyPhen-2 or SIFT. However, it is known that these prediction programs have significant false positive and negative rates and frequently do not agree with one another[34,35]. We therefore employed Fisher's exact test to estimate the probability that the p.Glu257Lys variant causes disease. This analysis showed that the allele frequency for the p.Glu257Lys variant was significantly higher in the LCA cases (6/568 chromosomes = 1.056%) compared to both our controls (0/1,002 chromosomes = 0%; $P = 0.002$) and ESP samples (13/10,758 chromosomes = 0.121%; $P = 0.0002$), which is consistent with a high likelihood that this variant is pathogenic.

To determine whether *NMNAT1* mutations cause LCA in other families, we sequenced *NMNAT1* in 56 unrelated probands with LCA evaluated at The Children's Hospital of Philadelphia (CHOP) and the Massachusetts Eye and Ear Infirmary (MEEI). We found rare compound heterozygous mutations in *NMNAT1* that segregated with disease in family 007, in which the proband was a 5-year-old girl with isolated LCA and there was no family history of the disease (**Fig. 1c** and **Table 1**). We also identified compound heterozygous variants in *NMNAT1* that segregated with disease in family 053, in which the proband was a 20-year-old man with LCA (**Fig. 1d** and **Table 1**). The four *NMNAT1* variants identified in these subjects were not identified in 501 control samples.

To investigate the frequency of *NMNAT1* mutations in LCA, we screened additional populations of affected individuals from varying ancestry groups. This analysis included 228 additional probands ascertained at Institut de la Vision in Paris, LVPEI in India and University College London (UCL). These analyses identified homozygous or compound heterozygous mutations in *NMNAT1* in 11 additional families with LCA (**Table 1** and **Supplementary Fig. 2**). All of the mutations detected are rare, and all, with the exception of one encoding the p.Glu257Lys variant, were predicted to be damaging by PolyPhen-2 and/or SIFT (**Table 1**). None of the *NMNAT1* variants identified in these subjects were identified by Sanger sequencing in 501 control samples. Review of available clinical information for individuals in whom *NMNAT1* mutations were identified as the cause of LCA (**Supplementary Note**) indicated that the majority have atrophic macular lesions (**Fig. 2**).

NMNAT1 encodes a rate-limiting enzyme that generates NAD^+, both in a biosynthetic pathway from nicotinic acid mononucleotide (NaMN) and in a salvage pathway from nicotinamide mononucleotide (NMN) (**Supplementary Fig. 3**)[21]. Three functionally nonredundant mammalian NMNAT isoforms encoded by different genes have been identified within distinct cellular compartments, with NMNAT1, NMNAT2 and NMNAT3 localizing to the nucleus, Golgi complex and mitochondria, respectively[5,22]. The mitochondrial isoform, NMNAT3, regenerates NAD^+ for cellular energetics, whereas NMNAT1 is involved in the nuclear NAD^+ homeostasis that is necessary for both DNA metabolism and cell signaling[5]. Of interest, Nmnat1 is the principal component of the mouse Wallerian degeneration fusion protein (Wld^S), which also includes a 70-residue N-terminal sequence from the Ube4b multiubiquitination factor, and has been shown to have neuroprotective activity[23]. Homozygous *Nmnat1*-knockout mice are embryonic lethal, whereas heterozygous *Nmnat1*-knockout mice have normal development[24]. Loss of *nmnat* in *Drosophila melanogaster* photoreceptors leads to photoreceptor cell degeneration[25].

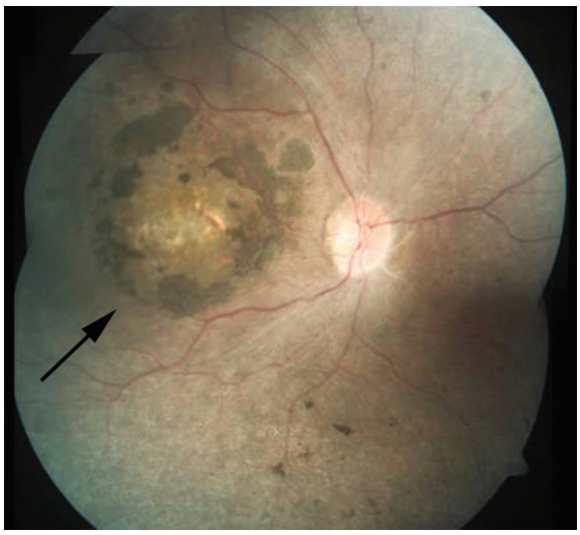

Figure 2 Retinal image from individual with LCA due to mutations in *NMNAT1*. Composite fundus image of the right eye of subject II-1 from LVPEI family LCA-100, showing pallor of the optic disc, attenuation of the retinal blood vessels, pigment disruption, atrophic changes in the macula (arrow) and scattered pigment clumping in the peripheral retina. The optic disc is ~1.75 mm in diameter.

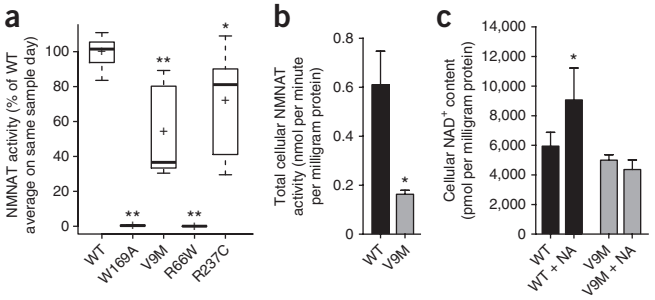

Figure 3 NMNAT1 enzyme activity and cellular NAD+ content. (**a**) The NAD+ biosynthetic activities of wild-type (WT) and mutant purified recombinant NMNAT1 proteins were measured. Box plots show activity measurements from replicate protein preparations that were independently generated and measured. The length of the box represents the 25th to 75th interquartile range, the interior horizontal line represents the median, the interior cross represents the mean, and vertical lines issuing from the box extend to the minimum and maximum values of the analysis variable. The p.Trp169Ala mutant had no NMNAT1 enzyme activity ($n = 6$; $P = 0.0014$), as was previously reported[32]. The p.Val9Met mutant had significantly lower enzyme activity (37% of wild-type NMNAT1 activity) ($n = 7$; $P = 0.0015$). The p.Arg237Cys mutant had 81% of wild-type NMNAT1 activity ($n = 6$; $P = 0.034$). The p.Arg66Trp mutant had no NMNAT1 enzyme activity ($n = 6$; $P = 0.0014$). $^*P < 0.05$; $^{**}P < 0.01$; determined by non-parametric Wilcoxon rank-sum test. (**b**) Total cellular NMNAT enzyme activity was measured in whole-cell extracts of fibroblasts from a healthy control and a proband with LCA (subject IV-1 from family 047) who was homozygous for the p.Val9Met NMNAT1 variant. The mutant cells had 27% of the total cellular NMNAT NAD+ synthetic activity of control cells (two-tailed *t* test $P = 0.016$; $n = 6$ for wild-type, $n = 5$ for mutant cells). (**c**) Cellular NAD+ levels. Total cellular NAD+ content was quantified by HPLC in the same control and mutant fibroblasts as in **b** at baseline and after exposure to 10 mM nicotinic acid (NA) for 24 h. NAD+ content in fibroblasts from the proband with LCA was decreased by 16% relative to that in wild-type cells ($P = 0.067$). Nicotinic acid exposure significantly increased NAD+ content in control cells but had no effect on NAD+ content in the mutant cells. $n = 7$ for both cell lines without treatment, $n = 6$ for control cells exposed to nicotinic acid, and $n = 4$ for mutant cells exposed to nicotinic acid. In **b** and **c**, data are shown as the mean with standard error; $^*P < 0.05$.

We assessed the potential deleterious effects of the novel missense variants p.Val9Met, p.Arg66Trp and p.Arg237Cys on the NMNAT1 protein. These altered residues are located in conserved regions of the protein (**Supplementary Fig. 4**) and are predicted to damage NMNAT1 protein structure and stability by several prediction programs[26,27]. All three of these mutant proteins showed correct nuclear localization and normal expression levels following expression of recombinant NMNAT1 proteins in heterologous cells (**Supplementary Fig. 5a**,**b**). In addition, the p.Val9Met mutant correctly localized to the nucleus of a fibroblast cell line obtained from the proband with LCA in family 047 (**Fig. 1a**, subject IV-1, and **Supplementary Fig. 5c**)[22].

Given the normal nuclear localization and expression of the mutant NMNAT1 proteins, we postulated that the deleterious effect of the p.Val9Met, p.Arg66Trp and p.Arg237Cys variants might be on NMNAT1 enzymatic function. We therefore measured the NAD+ biosynthetic activity of wild-type and mutant purified recombinant NMNAT1 proteins (**Fig. 3a**). Despite variability in enzyme rates between experimental days, the protein activity of the NMNAT1 p.Val9Met variant was reproducibly and significantly lower than that of wild-type protein on the same day (63.4% median reduction, interquartile range 31.4–88.7; Wilcoxon rank-sum test $P = 0.0015$). The enzyme activity of the p.Arg66Trp mutant was also significantly lower (99.5% median reduction, interquartile range 0.01–0.11; Wilcoxon rank-sum test $P = 0.0014$), although we were not able to achieve effective purification of the Flag-tagged version of this mutant (**Supplementary Fig. 6**), despite its clearly normal expression and nuclear localization in CHO and mIMCD3 cells (**Supplementary Fig. 5**). The enzyme activity of the p.Arg237Cys mutant was only marginally lower than that of wild-type protein (18.9% reduction, interquartile range 41.1–90.1; Wilcoxon rank-sum test $P = 0.034$) (**Fig. 3a**), raising the question of how this mutation causes disease. It has been observed that NMNAT1 forms functional homo-oligomers and that amino acids 234–238 participate in these protein interactions[5]. To evaluate whether the pathogenic effect of the p.Arg237Cys alteration could be related to its location in a region of NMNAT1 that is involved in protein multimerization, we measured NMNAT1 activity in recombinant protein purified from cells cotransfected with constructs for both the p.Arg66Trp and p.Arg237Cys variants that were identified in family 007. We observed notably lower enzyme activity (18% of wild-type control rate; data not shown) in the combined protein preparation. Additional studies using extracts from the fibroblast cells of the proband with the p.Val9Met alteration (**Fig. 1a**, subject IV-1) showed 73% lower total cellular NMNAT enzyme activity (two-tailed *t* test $P = 0.016$) relative to wild-type control (**Fig. 3b**). These data suggest that the pathogenic effects of these mutations are related, at least in part, to significantly reduced NMNAT1 enzyme activity. It will be of interest to investigate the function of the mutant NMNAT1 proteins in retinal cells, given the isolated retinal phenotype of LCA.

The total NAD+ concentration of human cells has many contributing determinants[21,28]. We measured NAD+ in the fibroblast cell line from the proband with LCA (**Fig. 1a**, subject IV-1) to determine whether the p.Val9Met alteration in the nuclear-localized NMNAT1 protein significantly affected total cellular NAD+ content. Fibroblasts from the proband with LCA had 16% less NAD+ content than wild-type controls, although this difference was not statistically significant (two-tailed *t* test $P = 0.067$; **Fig. 3c**). These data suggest that the reduction in NMNAT1 enzyme activity caused by the p.Val9Met alteration may be sufficient to affect total cellular NAD+ content.

Cellular NAD+ concentrations can be directly increased by nicotinic acid, which requires NMNAT activity for its conversion to NAD+ (**Supplementary Fig. 3**)[29]. We therefore asked whether cellular NAD+ concentration in the fibroblasts expressing the NMNAT1 p.Val9Met mutant (from subject IV-1) was altered by exposure to 10 mM nicotinic acid for 24 h. Notably, whereas nicotinic acid significantly increased the total cellular NAD+ content by 53% in control cells (two-tailed *t* test $P = 0.021$), it had no effect on NAD+ content in the fibroblasts from the proband with LCA (**Fig. 3c**; two-tailed *t* test $P > 0.05$). The inability of nicotinic acid to increase the NAD+ content in NMNAT1 p.Val9Met mutant fibroblasts provides further evidence that they have a substantial deficiency in cellular NMNAT enzymatic activity.

In summary, we report here the first instance of disease association with an NMNAT isoform[5]. *NMNAT1* mutations cause LCA and are the likely pathogenic basis for disease previously linked to the LCA9 locus, although the family in which disease was originally linked to this locus was not available for analysis in this study[4] (C. Toomes and C. Inglehearn, personal communication). Through exome sequencing in a consanguineous Pakistani kindred with LCA and subsequent Sanger sequencing of *NMNAT1* in 284 additional unrelated probands with LCA, we identified mutations in 14 unrelated

families (14/285 = 4.9% of unrelated cases). This work suggests that mutations in *NMNAT1* are a relatively common cause of LCA[3]. However, because the cohorts of individuals used for these studies are enriched for subjects without mutations in known LCA-causing genes, the proportion of all LCA cases caused by *NMNAT1* mutations is likely to be overestimated by these data.

The identification of *NMNAT1* as an LCA-causing gene raises the intriguing question of how mutations in a widely expressed NAD^+ biosynthetic protein lead to a retina-specific phenotype. The data presented suggest that the retinal degeneration phenotype observed in individuals with *NMNAT1* mutations results from decreased NAD^+ biosynthetic activity. This hypothesis is consistent with findings from studies of the Wld^S protein in mice, which showed that the neuroprotective effect of the Wld^S protein required both the Ube4b component and an enzymatically active NMNAT1 portion of the chimeric protein[30]. However, it seems that, in some systems, such as *Drosophila*, *nmnat* alone has a neuroprotective role that may be independent of its NAD^+ biosynthetic activity[25,31]. Thus, it remains to be determined whether retinal degeneration caused by mutations in *NMNAT1* results primarily from the loss of a potentially novel neuroprotective effect of NMNAT1 or a previously unappreciated role of NAD^+-mediated signaling in retinal health and disease. In either case, *NMNAT1* mutations represent a new pathophysiological cause of LCA, further underscoring the genetic heterogeneity of inherited retinal diseases[3,6]. We postulate that pharmacologic and/or genetic therapies directed at restoring cellular NAD^+ homeostasis in retinal cells may offer a therapeutic strategy for *NMNAT1*-related LCA.

URLs. Exome Variant Server, NHLBI Exome Sequencing Project (ESP), http://evs.gs.washington.edu/EVS/; RetNet Retinal Information Network, https://sph.uth.tmc.edu/retnet/; 1000 Genomes Project, http://www.1000genomes.org/; UCSC Genome Browser, http://genome.ucsc.edu/.

METHODS

Methods and any associated references are available in the online version of the paper.

Accession codes. Exome sequence data for family 047 is available at the NCBI Sequence Read Archive (SRA) under accession SRP013517.

Note: Supplementary information is available in the online version of the paper.

ACKNOWLEDGMENTS

We thank M. Sousa, D. Harnley, M.-E. Lancelot and A. Antonio for their excellent technical assistance, The Children's Hospital of Philadelphia CytoGenomics Laboratory for assistance with the establishment of the fibroblast cell lines and tissue culture and J. Baur for his helpful discussions on NAD^+ metabolism. We are grateful to the individuals with LCA and their relatives for their participation in this study.

This work was supported by grants from the US National Institutes of Health (RO1-EY12910 (E.A.P.), R03-DK082446 (M.J.F.), R01-GM097409 (E.N.-O.), P30HD026979 (M.J.F. and R.X.) and P30EY014104 (Massachusetts Eye and Ear Infirmary core support)); the Foundation Fighting Blindness USA (I.A., A.D.B., E.L.B., S.S.B., Q.L., A.T.M., D.S.M., E.A.P., J.-A.S., S.M.-S. and A.R.W.); the Rosanne Silbermann Foundation (E.A.P.); the Penn Genome Frontiers Institute (E.A.P. and X.G.); the Institutional Fund to the Center for Biomedical Informatics by the Loyola University Stritch School of Medicine (X.G.); the Foerderer Award for Excellence from the Children's Hospital of Philadelphia (M.J.F. and X.G.); the Angelina Foundation Fund from the Division of Child Development and Metabolic Disease at the Children's Hospital of Philadelphia (M.J.F.); the Clinical and Translational Research Center at the Children's Hospital of Philadelphia (UL1-RR-024134) (M.J.F. and E.A.P.); the Department of Biotechnology, the Government of India and the Champalimaud Foundation, Portugal (C.K.); the Hyderabad Eye Research Foundation (C.K.); a senior research fellowship from the Council for Scientific and Industrial Research (R.S.); the Foundation Voir et Entendre, Ville de Paris and Région Ille de France (C.Z.); RP Fighting Blindness (UK)(A.R.W.); Fight For Sight (UK) (A.D.B., S.S.B., A.T.M., D.S.M. and A.R.W.); Moorfields Eye Hospital National Institute of Health Research (NIHR) British Research Council (BRC) for Ophthalmology (A.D.B., S.S.B., A.T.M., D.S.M. and A.R.W.); and the Special Trustees of Moorfields Eye Hospital (A.D.B., S.S.B., A.T.M., D.S.M. and A.R.W.). The content is solely the responsibility of the authors and does not necessarily represent the official views of the funding organizations or the National Institutes of Health. This project is funded, in part, by the Penn Genome Frontiers Institute under a grant with the Pennsylvania Department of Health, which disclaims responsibility for any analyses, interpretations or conclusions.

AUTHOR CONTRIBUTIONS

Experiments were designed by Q.Z., M.J.F., X.G. and E.A.P. LCA case samples and controls were provided by I.A., A.D.B., E.L.B., S.S.B., C.K., M.J.F., S.J., A.T.M., E.P., S.M.-S., J.-A.S., A.R.W. and E.A.P. Pedigrees were compiled by A.D.B., C.C., C.K., S.J. and E.P. Individuals III-4, III-5, IV-1, IV-2 and IV-3 were clinically evaluated by M.J.F. and E.A.P. (individuals III-3, III-6 and IV-4 to IV-7 were not clinically evaluated by the authors). Exome sequencing was performed by M.C. Bioinformatics pipeline development was performed by X.G., M.J.F., E.A.P. and M.C. Exome data analyses were performed by J.C.P., X.G., Z.F.-K. and E.A.P. *NMNAT1* sequencing and segregation analyses were performed by I.A., C.C., M.C., Z.F.-K., D.S.M., L.P., R.S., N.H.W., C.Z. and Q.Z. High-performance liquid chromatography (HPLC)-based NMNAT enzyme activity assay and NAD^+ content assay development was performed by E.N.-O., with data analysis performed by E.N.-O., M.J.F., E.A.P. and R.X. *In vitro* functional studies were carried out by Q.Z., E.N.-O., J.O., Q.L. and M.S. The manuscript was written by M.J.F., Q.Z., X.G. and E.A.P.

COMPETING FINANCIAL INTERESTS

The authors declare no competing financial interests.

Published online at http://www.nature.com/doifinder/10.1038/ng.2361.
Reprints and permissions information is available online at http://www.nature.com/reprints/index.html.

1. Weleber, R.G. Infantile and childhood retinal blindness: a molecular perspective. *Ophthalmic Genet.* **23**, 71–97 (2002).
2. Michaelides, M., Hardcastle, A.J., Hunt, D.M. & Moore, A.T. Progressive cone and cone-rod dystrophies: phenotypes and underlying molecular genetic basis. *Surv. Ophthalmol.* **51**, 232–258 (2006).
3. den Hollander, A.I., Black, A., Bennett, J. & Cremers, F.P. Lighting a candle in the dark: advances in genetics and gene therapy of recessive retinal dystrophies. *J. Clin. Invest.* **120**, 3042–3053 (2010).
4. Keen, T.J. *et al.* Identification of a locus (LCA9) for Leber's congenital amaurosis on chromosome 1p36. *Eur. J. Hum. Genet.* **11**, 420–423 (2003).
5. Lau, C., Niere, M. & Ziegler, M. The NMN/NaMN adenylyltransferase (NMNAT) protein family. *Front. Biosci.* **14**, 410–431 (2009).
6. Pierce, E.A. Pathways to photoreceptor cell death in inherited retinal degenerations. *Bioessays* **23**, 605–618 (2001).
7. Daiger, S.P., Bowne, S.J. & Sullivan, L.S. Perspective on genes and mutations causing retinitis pigmentosa. *Arch. Ophthalmol.* **125**, 151–158 (2007).
8. Maguire, A.M. *et al.* Safety and efficacy of gene transfer for Leber's congenital amaurosis. *N. Engl. J. Med.* **358**, 2240–2248 (2008).
9. Bainbridge, J.W. *et al.* Effect of gene therapy on visual function in Leber's congenital amaurosis. *N. Engl. J. Med.* **358**, 2231–2239 (2008).
10. Cideciyan, A.V. *et al.* Human gene therapy for RPE65 isomerase deficiency activates the retinoid cycle of vision but with slow rod kinetics. *Proc. Natl. Acad. Sci. USA* **105**, 15112–15117 (2008).
11. Maguire, A.M. *et al.* Age-dependent effects of *RPE65* gene therapy for Leber's congenital amaurosis: a phase 1 dose-escalation trial. *Lancet* **374**, 1597–1605 (2009).
12. Jacobson, S.G. *et al.* Gene therapy for Leber congenital amaurosis caused by *RPE65* mutations: safety and efficacy in 15 children and adults followed up to 3 years. *Arch. Ophthalmol.* **130**, 9–24 (2012).
13. Sherry, S.T. *et al.* dbSNP: the NCBI database of genetic variation. *Nucleic Acids Res.* **29**, 308–311 (2001).
14. 1000 Genomes Project Consortium. A map of human genome variation from population-scale sequencing. *Nature* **467**, 1061–1073 (2010).
15. Grant, G.R. *et al.* Comparative analysis of RNA-Seq alignment algorithms and the RNA-Seq unified mapper (RUM). *Bioinformatics* **27**, 2518–2528 (2011).
16. Ramensky, V., Bork, P. & Sunyaev, S. Human non-synonymous SNPs: server and survey. *Nucleic Acids Res.* **30**, 3894–3900 (2002).
17. Ng, P.C. & Henikoff, S. SIFT: predicting amino acid changes that affect protein function. *Nucleic Acids Res.* **31**, 3812–3814 (2003).

18. Sullivan, L.S. *et al.* Prevalence of disease-causing mutations in families with autosomal dominant retinitis pigmentosa: a screen of known genes in 200 families. *Invest. Ophthalmol. Vis. Sci.* **47**, 3052–3064 (2006).
19. Stone, E.M. Leber congenital amaurosis—a model for efficient genetic testing of heterogeneous disorders: LXIV Edward Jackson Memorial Lecture. *Am. J. Ophthalmol.* **144**, 791–811 (2007).
20. Wang, M. & Marin, A. Characterization and prediction of alternative splice sites. *Gene* **366**, 219–227 (2006).
21. Belenky, P., Bogan, K.L. & Brenner, C. NAD^+ metabolism in health and disease. *Trends Biochem. Sci.* **32**, 12–19 (2007).
22. Berger, F., Lau, C., Dahlmann, M. & Ziegler, M. Subcellular compartmentation and differential catalytic properties of the three human nicotinamide mononucleotide adenylyltransferase isoforms. *J. Biol. Chem.* **280**, 36334–36341 (2005).
23. Coleman, M.P. & Freeman, M.R. Wallerian degeneration, wld^S, and nmnat. *Annu. Rev. Neurosci.* **33**, 245–267 (2010).
24. Conforti, L. *et al.* Reducing expression of NAD^+ synthesizing enzyme NMNAT1 does not affect the rate of Wallerian degeneration. *FEBS J.* **278**, 2666–2679 (2011).
25. Zhai, R.G. *et al. Drosophila* NMNAT maintains neural integrity independent of its NAD synthesis activity. *PLoS Biol.* **4**, e416 (2006).
26. Siepel, A. *et al.* Evolutionarily conserved elements in vertebrate, insect, worm, and yeast genomes. *Genome Res.* **15**, 1034–1050 (2005).
27. Worth, C.L., Preissner, R. & Blundell, T.L. SDM—a server for predicting effects of mutations on protein stability and malfunction. *Nucleic Acids Res.* **39**, W215–W222 (2011).
28. Bogan, K.L. & Brenner, C. Nicotinic acid, nicotinamide, and nicotinamide riboside: a molecular evaluation of NAD^+ precursor vitamins in human nutrition. *Annu. Rev. Nutr.* **28**, 115–130 (2008).
29. Nikiforov, A., Dolle, C., Niere, M. & Ziegler, M. Pathways and subcellular compartmentation of NAD biosynthesis in human cells: from entry of extracellular precursors to mitochondrial NAD generation. *J. Biol. Chem.* **286**, 21767–21778 (2011).
30. Conforti, L. *et al.* Wld^S protein requires Nmnat activity and a short N-terminal sequence to protect axons in mice. *J. Cell Biol.* **184**, 491–500 (2009).
31. Avery, M.A., Sheehan, A.E., Kerr, K.S., Wang, J. & Freeman, M.R. Wld^S requires Nmnat1 enzymatic activity and N16-VCP interactions to suppress Wallerian degeneration. *J. Cell Biol.* **184**, 501–513 (2009).
32. Berger, F., Lau, C. & Ziegler, M. Regulation of poly(ADP-ribose) polymerase 1 activity by the phosphorylation state of the nuclear NAD biosynthetic enzyme NMN adenylyl transferase 1. *Proc. Natl. Acad. Sci. USA* **104**, 3765–3770 (2007).
33. den Hollander, A.I., Roepman, R., Koenekoop, R.K. & Cremers, F.P. Leber congenital amaurosis: genes, proteins and disease mechanisms. *Prog. Retin. Eye Res.* **27**, 391–419 (2008).
34. Chun, S. & Fay, J.C. Identification of deleterious mutations within three human genomes. *Genome Res.* **19**, 1553–1561 (2009).
35. Wei, Q., Wang, L., Wang, Q., Kruger, W.D. & Dunbrack, R.L. Jr. Testing computational prediction of missense mutation phenotypes: functional characterization of 204 mutations of human cystathionine β synthase. *Proteins* **78**, 2058–2074 (2010).

ONLINE METHODS

Subject recruitment and clinical evaluations. The clinical study was approved by the institutional review boards of The Massachusetts Eye and Ear Infirmary, the Children's Hospital of Philadelphia, Comité de Protection des Personnes (CDP) Ile de France V, the LV Prasad Eye Hospital and University College London, and conformed to the tenets of the Declaration of Helsinki. Informed consent was obtained from the participants. Complete ophthalmic and clinical genetic evaluations of members of family 047 (subjects IV-1, IV-1 and IV-3), family 007 (subject II-2) and family 053 were performed at the Ophthalmology-Genetics Clinic at the Children's Hospital of Philadelphia.

Exome sequencing. Exome capture was performed using the SureSelect 50 Mb All Exon Targeted Enrichment kit from Agilent Technologies in accordance with the kit manual[36]. The resulting exome-capture libraries underwent 2 × 101-bp paired-end sequencing on an Illumina HiSeq 2000 Next-Generation Sequencing system using v2.5 SBS chemistry, with average flow-cell lane cluster densities of ~800,000/mm^2. One exome sample was analyzed per flow-cell lane to obtain a minimum of 10× read depth for 92–95% of the targeted exome.

Exome data analyses. Burrows-Wheeler Aligner (BWA, version 0.5.9-r16) was used to align the sequence reads to the human reference genome GRCh37 downloaded from the 1000 Genomes Project website (see URLs)[37]. SAMtools (version 0.1.12 or r859) was used to remove potential duplicates (with the rmdup command) and to make initial SNP and insertion and/or deletion (indel) calls (with the pileup command)[38]. A custom program was developed and used to further refine the SNP and indel calls. The custom program used a false discovery rate approach to adjust raw base counts at a candidate position after Benjamini-Hochberg correction was performed using quality values of all bases[39]. A coverage depth cutoff of 10× was then applied. The fraction of a variant base had to be between 0.25 and 0.75 to be called heterozygous and above 0.75 to be called homozygous. Resulting variant calls were annotated using our custom human base-pair codon database. This database maps each base position in the human reference genome on the basis of Ensembl Release 65 gene annotations to its corresponding transcripts, genes, codons, encoded amino acids and translation frames, if any. Additional annotations of each variant call were provided using data sets downloaded from the 1000 Genomes Project website, the NHLBI Exome Sequencing Project Exome Variant Server and the UCSC Genome Browser (see URLs). These annotations include allele frequencies, SIFT and PolyPhen predictions, and phastCons conservation scores[16,17]. Custom scripts were also developed and used to identify candidate variants that fit different filtering criteria, such as genetic models.

***NMNAT1* PCR amplification, Sanger sequencing and genotype confirmation.** Subjects in families 007 and 047 and probands from other families with LCA were selected for Sanger sequence analysis using primers to amplify all four exons and intron-exon boundaries of *NMNAT1* (**Supplementary Table 1**). PCR products were sequenced with the ABI PRISM BigDye Terminator Cycle Sequencing V2.0 Ready Reaction kit on an ABI 3100 or 3730 DNA analyzer (Applied Biosystems). To genotype the members of family 047, the relevant PCR product was digested with AcuI, which cuts the wild-type but not the mutant sequence.

Human fibroblast culture and exposure to nicotinic acid. Skin biopsies were performed on two siblings with LCA and their parents (**Fig. 1a**, subjects IV-1, IV-3, III-4 and III-5) after informed consent was obtained in accordance with the protocol approved by the institutional review board of the Children's Hospital of Philadelphia (08-6177, M.J.F.). Fibroblast cell lines were established in the CytoGenomics Laboratory at the Children's Hospital of Pennsylvania and were subsequently maintained in T75 flasks in a 37 °C CO_2 incubator, per standard protocol, in DMEM (Gibco) supplemented with 20% FBS, 2 mM L-glutamine, 1 mM pyruvate and 50 μg/ml uridine (Calbiochem). Cells were grown to confluence before undergoing functional analyses. Cells in T75 flasks were exposed to 10 mM nicotinic acid (Sigma) for 24 h and were trypsinized, washed twice with Hank's balanced salt solution (Gibco) and flash frozen in liquid nitrogen for HPLC analysis.

Cell culture. CHO-K1 and wild-type mIMCD3 cell lines were purchased from the American Type Culture Collection (ATCC). mIMCD3 cells were maintained in DMEM:F12 medium supplemented with 10% FBS and 0.5 mM sodium pyruvate. CHO cell culture was performed in F12 medium supplemented with 10% FBS. Transfection was performed with Lipofectamine 2000 (Invitrogen), and cells were processed for immunocytochemistry 48–72 h after transfection. Human skin fibroblast cells obtained from two siblings with LCA (**Fig. 1a**, subjects IV-1 and IV-3) and their parents (**Fig. 1a**, subjects III-IV and III-V) were maintained in Medium 106 (Invitrogen) with low-serum growth supplement and were grown to confluence before undergoing immunofluorescence and immunoblot analyses.

Immunofluorescence analyses. Cells were fixed in 4% paraformaldehyde, permeabilized and then blocked with 1% BSA and 0.2% Triton X-100 in PBS, as previously described[40]. Cells were then stained with antibody to V5 (Invitrogen, 46-0705; 1:1,000 dilution) and then with Alexa Fluor 555–conjugated goat secondary antibody to mouse IgG (Invitrogen, A21127; 1:1,000 dilution)[40]. Fluorescent signals were visualized using a Nikon Eclipse fluorescent microscope.

Protein blotting. Total cell lysates from CHO cells transfected with pCAG-V5-*NMNAT1*-IRES-*EGFP* plasmid were separated on a precast NuPAGE 4–12% Bis-Tris Gel (Invitrogen) and were transferred to a PVDF membrane, as previously described[41]. The membrane was probed with antibody to V5 (Invitrogen, 46-0705; 1:5,000 dilution), human NMNAT1 (Novus Biologicals, H00064802-B01P; 1:500 dilution) or β-actin (Santa Cruz Biotechnology, sc-1615; 1:1,000 dilution) and was then incubated with IRDye secondary antibodies (LI-COR, goat anti-mouse 800CW, 926-32210; goat anti-rabbit 680RD, 926-68071; 1:15,000 dilutions). Antibody binding was detected with an Odyssey infrared imager (LI-COR).

Recombinant protein production and purification. Human *NMNAT1* cDNA was amplified by RT-PCR from a cDNA clone (OpenBiosystem) and cloned into a pENTR/D-TOPO entry vector (Invitrogen); the construct was fully verified by sequencing. The coding sequence was moved by recombination to a Gateway-compatible destination expression vector modified to encode a sequence for N-terminal V5 (pCAG-V5-IRES-*EGFP*) or Flag (pCAG-Flag-IRES-*EGFP*) epitope tags in frame. Plasmid DNA was purified using the EndoFree plasmid maxi kit (Qiagen). Recombinant NMNAT1 (with Flag tag) was expressed in CHO cells and was purified using a FLAG M Purification kit (Sigma) for subsequent enzyme activity assay.

NMNAT enzyme activity assay. NMNAT activity was measured by HPLC quantitation of the reaction product, NAD^+. The assay mixture contained 1.5 mM ATP, 1 mM NMN and 10 mM $MgCl_2$ in 25 mM Tris-HCl (pH 7.4) and the appropriate amount of enzyme sample (typically 20 or 40 μl) to achieve a final volume of 0.2 ml. The reaction was started by addition of NMN substrate. After incubation of the reaction mixture for 10, 30 or 120 min at 37 °C, a 40-μl aliquot was removed and added to 20 μl of ice-cold 1.2 M perchloric acid (PCA) containing 20 mM EDTA and 0.15% sodium metabisulfite to stop the reaction. After a 15-min incubation at 4 °C, the mixture was centrifuged for 10 min at 16,000*g* in a Beckman microcentrifuge. A 55-μl aliquot of the supernatant was further neutralized by the addition of 20 μl of ice-cold 1 M K_2CO_3 and was centrifuged again. The supernatant was isolated and stored at −80 °C until HPLC analysis.

Sample preparation for HPLC analyses of NAD^+. Harvested cells were rinsed with Hank's balanced salt solution twice and were centrifuged at 2,150*g* for 5 min. The cell pellet was resuspended in argon-bubbled 20 mM Tris-HCl (pH 7.4) for analysis of the oxidized dinucleotides, including NAD^+. The cell suspension was extracted with four volumes of argon-bubbled, ice-cold 1.2 M PCA containing 20 mM EDTA and 0.15% sodium metabisulfite. After vortexing, the suspension was placed on ice for 15 min and then centrifuged at 16,000*g* for 10 min. The supernatant was neutralized with 1 M potassium carbonate and was centrifuged to remove insoluble material. The pellet from the PCA extraction was used for protein estimation. Samples were stored at −80 °C and were subjected to HPLC analysis.

HPLC conditions for analyses of NAD^+. Separation of the oxidized dinucleotides was carried out on a C18 column (5 µm, 4.6 × 250 mm, Adsorbosphere XL C18 90Å) preceded by a guard column at 40 °C. Flow rate was set at 0.5 ml/min. The mobile phase was initially 100% of mobile phase A (0.1 M sodium phosphate buffer (pH 6.0) containing 3.75% methanol). The methanol concentration was linearly increased with mobile phase B (0.1 M sodium phosphate buffer (pH 6.0) containing 30% methanol), increasing to 50% over 15 min. The column was washed after each separation by increasing mobile phase B to 100% for 5 min. UV absorbance was monitored at 260 and 340 nm with Shimadzu SPD-M20A. Pertinent peak areas were integrated using LabSolution software from Shimadzu and were quantified using standard curves.

Statistical analyses. For comparison of the activity rates of purified recombinant NMNAT1 proteins with that of wild-type protein, rates were normalized by the mean rate of the wild-type protein analyzed on the same day to account for variation in the absolute enzyme activity rates on different analysis dates. The significance of differences between groups was evaluated using a nonparametric Wilcoxon rank-sum test in SAS 4.3 because of skewness observed in the data and small sample size. For measurements of cellular NMNAT activity and NAD^+ concentrations, statistical comparisons between groups were performed using Student's two-tailed *t*-tests.

36. Gnirke, A. *et al.* Solution hybrid selection with ultra-long oligonucleotides for massively parallel targeted sequencing. *Nat. Biotechnol.* **27**, 182–189 (2009).
37. Li, H. & Durbin, R. Fast and accurate short read alignment with Burrows-Wheeler transform. *Bioinformatics* **25**, 1754–1760 (2009).
38. Li, H. *et al.* The Sequence Alignment/Map format and SAMtools. *Bioinformatics* **25**, 2078–2079 (2009).
39. Benjamini, Y. & Hochberg, Y. Controlling the false discovery rate: a practical and powerful approach to multiple testing. *J. Royal Stat. Soc. B (Methodological)* **57**, 289–300 (1995).
40. Liu, Q., Zuo, J. & Pierce, E.A. The retinitis pigmentosa 1 protein is a photoreceptor microtubule-associated protein. *J. Neurosci.* **24**, 6427–6436 (2004).
41. Davis, E.E. *et al. TTC21B* contributes both causal and modifying alleles across the ciliopathy spectrum. *Nat. Genet.* **43**, 189–196 (2011).

doi:10.1038/ng.2361